Control of MMC-based Isolated DC/DC converter for HVDC Tapping

Zhang, Qi; Silva, Filipe Miguel Faria da; Irnawan, Roni; Mochamad, Rian

Published in:
2023 IEEE Belgrade PowerTech, PowerTech 2023

DOI (link to publication from Publisher):
10.1109/PowerTech55446.2023.10202693

Publication date:
2023

Document Version
Early version, also known as pre-print

Control of MMC-based Isolated DC/DC converter for HVDC Tapping

Qi Zhang
AAU Energy
Aalborg University
Aalborg, Denmark
qzg@energy.aau.dk

Filipe Faria da Silva
AAU Energy
Aalborg University
Aalborg, Denmark
ffs@energy.aau.dk

Roni Irnawan
Department of Ele. and Inf. Eng.
Gadjah Mada University
Yogyakarta, Indonesia
roniirnawan@ugm.ac.id

Rian Fatah Mochamad
Department of Ele. and Inf. Eng.
Gadjah Mada University
Yogyakarta, Indonesia
rianfatahm@gmail.com

***Abstract*—With development of HVDC technology, HVDC tapping technology becomes more attractive as a solution to improve reliability and power quality as well as to replace fossil fuels generation of tiny-scale island power systems. This paper proposes a modular multilevel converter (MMC) based isolated DC/DC converter as a potential solution for HVDC tapping technology, which extracts a small amount of energy from the main HVDC link to a low-voltage DC grid, to support a local island power system. Firstly, a new mathematical model of the isolated DC/DC converter is developed by introducing the common-mode and the difference-mode voltage. The developed model illustrates that the AC current can only be affected by the difference-mode voltage, and the power is simultaneously affected by the AC current and the common-mode voltage. Secondly, based on the developed model, a control system consisting of the current and the voltage control loops is designed for an MMC-based isolated DC/DC converter. The proposed control method is more flexible, and the dynamic performance of the isolated DC/DC converter can be improved by using the proposed method. A simulation verifies the performance of the proposed control system.**

***Index Terms*—HVDC Tapping, isolated DC/DC converter, control strategy**

I. Introduction

As the world's largest archipelagic country, Indonesia's power system is divided into many independent power systems by its unique geographical environment, with different voltage levels, topologies, and power generation sources [1], [2]. Such a decentralized and independent power system faces significant power system stability and reliability challenges [1], [2]. Meanwhile, considering the abundant renewable energy potential, Indonesia is looking to shift its coal dependency to renewable energy sources [2], however, the decentralized power system results in some issues in renewable energy integration, e.g., weak or very-weak grid conditions, long-distance power transmission, and randomness of renewable energy generation. Therefore, Aalborg University (AAU), Universitas Gadjah Mada (UGM), and Indonesian Electric Power Company PLN jointly conducted an HVDC GREEN project to investigate the possibility of the HVDC interconnection of various independent power systems.

The research is funded by the Ministry of Foreign Affairs of Denmark via the Danida Fellowship Centre with the project: *"HVDC GREEN: HVDC Grid for intErconnEcting Nusantara"*, project no. 20-M02AAU

Indonesia has many small islands far away from the large islands. Limited by the natural condition and economic development factors, these islands generally use small-scale power systems, which are very weak and have challenges in power system stability and power quality [1]–[3]. To improve stability and power quality, the HVDC GREEN project studies HVDC power tapping technology to support these island power systems. The HVDC power tapping aims to utilize a DC/DC converter, namely tapping converters, as an interface to extract a small amount of energy from the main HVDC link to support the island power system. Furthermore, it is assumed that these island power systems only draw electric power from the HVDC link because of the limited power generation capacity. To meet requirements of HVDC tapping technology, this paper proposes a potential solution for tapping converters, including topology and control system design.

Accompanied by the fast and comprehensive development of the HVDC transmission system, high-power DC/DC converters have gradually attracted research attentions. Many DC/DC converters with different topologies and control strategies have been proposed. Generally, those proposed converters can be divided into isolated or non-isolated converters according to circuit topologies [4]. The isolated DC/DC converter utilizes medium- or high-frequency transformers isolating two DC terminals to give more flexibility on the grounding configuration and to maintain security requirements [5]. Therefore, the isolated DC/DC converter is a feasible solution for HVDC power tapping.

Literature [6] proposes an isolated MMC-based DC/DC converter containing a medium transformer with a ratio of three, and two MMCs generating square-wave AC voltage, similar with traditional dual-active-bridge (DAB) DC/DC converters. Modulation methods, power balancing strategies of MMC submodules, and phase-shift-based DC power flow control are studied in this reference. Meanwhile, [7] compares three variants of DAB DC/DC converters regarding power balancing, design consideration, and power losses. However, these DC/DC converters are not a very good solution for high-voltage applications. The square wave AC voltage contains many harmonics and may produce high iron losses in the transformer. Furthermore, the phase-shift control strategy cannot deal with reactive power balance for the DC/DC converter

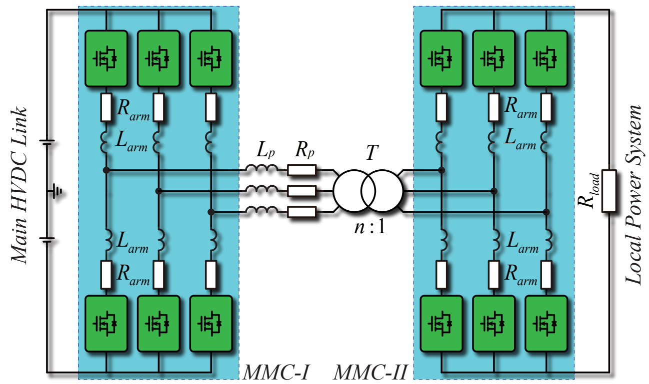

Fig. 1. The topology of the MMC-based isolated DC/DC converter

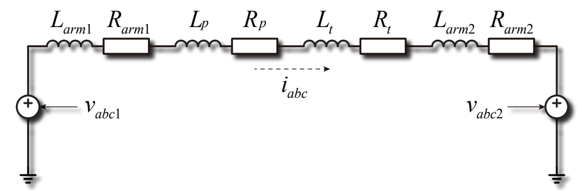

Fig. 2. The representation of the isolated DC/DC converter under per-unit system

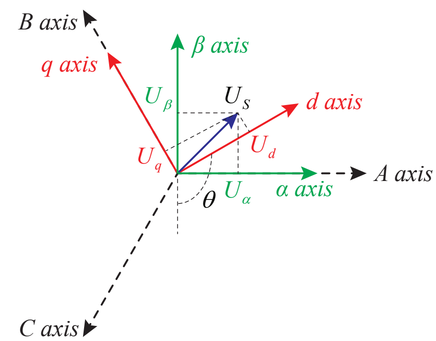

Fig. 3. The illustration of DQ transform definition.

desired in HVDC tapping. It has been pointed out that the sine wave-based DC/DC isolated converter is more suitable for high-power applications [8] because of the harmonics, switching losses, and power balancing between two DC/AC converters [9], [10].

An MMC-based, isolated DC/DC converter is proposed in [5]. It firstly develops a mathematical model of DC/DC converters in the phasor domain, and then, a dual channel control strategy with fault ride-through capability is proposed for the DC/DC converter. The DC/DC converter in [5] utilizes the sine-wave AC voltage for the transformer, and it uses a fixed modulation index for both DC/AC converters. Because of the fixed modulation, the AC voltage generated by DC/AC converters can be directly affected by DC voltage. In other words, if the DC output voltage is disturbed and has a variation, the AC voltage will simultaneously and directly reflect the disturbance, so that the power delivered will be affected also. Therefore, the dual channel control strategy is suitable for the DC/DC converter used for power flow controller where DC voltages of two terminals are constant. However, the performance of the dual channel control strategy may become worse in the case that output DC voltage is a control objective.

In order to overcome the disadvantages mentioned above of isolated DC/DC converters, this paper aims to propose an MMC-based isolated DC/DC converter for HVDC power tapping applications. Firstly, this paper develops the dynamic model of an MMC-based isolated DC/DC converter. Secondly, the control system based on difference-mode and common-mode voltage is designed for the converter working in voltage control mode. Finally, performance of the proposed control strategy is demonstrated with the simulation in PSCAD.

II. Topology and Model of the Isolated DC/DC Converter

Fig. 1 illustrates essential elements of the studied DC/DC converter consisting of two MMC converters, a three-phase power inductor, and a three-phase transformer. The MMC-I connected to the main HVDC link generates a controllable medium frequency AC voltage for the step-down transformer isolating the main HVDC link from the local low-voltage DC system. The MMC-II, controlled as a rectifier, provides stable low-level DC voltage for the local area. The three-phase power inductor is used here to provide impedance for the power control, as discussed in following section.

A. Modeling of the studied DC/DC converter

Modelling of the studied converter could be more straightforward using per-unit system. Define the base voltage of two terminals of the transformer as rate voltages V_{b1} and V_{b2}, respectively for MMC-I and MMC-II sides, and the rated power of the DC/DC converter as S_b. With the above definition, the studied DC/DC converter can be represented as in Fig. 2 by applying per-unit system. The MMC is represented by two controllable voltage sources, which means that this study ignores the inner dynamic and energy balancing of MMC's sub-models (SMs), and it assumes that the MMC are well-controlled in the low-level control. In other words, this study only considers high-level control in terms of the current control loop and the power control loop. In the figure, the $L_{arm1}, R_{arm1}, L_{arm2}, R_{arm2}$ represent the arm inductors, resistors of MMC-I and MMC-II, respectively. Moreover, L_t, R_t are used to represent the equivalent inductor and resistor of the leakage inductance and winding losses. The L_p, R_p represent the inductance and resistance of the power filter. Positive direction of three-phase current is defined as from the MMC-I to the MMC-II.

B. Inductor Current Model

For isolated DC/DC converters, active power is controlled by adjusting AC current flowing through the three-phase inductor and voltages of AC terminals of two MMC blocks.

Therefore, the control of inductor current is a fundamental part of the control system design of the tapping converter. Because of AC voltage and current in the system, it is much more convenient to analyze the system using DQ transform. The definition of the DQ transform used in this study is shown in Fig. 3 and (1).

$$\boldsymbol{T_{dq}(\theta)} = \frac{2}{3}\begin{bmatrix} \sin(\theta) & \sin(\theta-\frac{2\pi}{3}) & \sin(\theta+\frac{2\pi}{3}) \\ \cos(\theta) & \cos(\theta-\frac{2\pi}{3}) & \cos(\theta+\frac{2\pi}{3}) \\ \frac{1}{2} & \frac{1}{2} & \frac{1}{2} \end{bmatrix} \quad (1)$$

Denote the per-unit value of three-phase voltage generated by MMC-I and MMC-II as v_{abc1}, v_{abc2}, respectively. According to the representation of the studied DC/DC converter shown in Fig. 2, the mathematical model of the DC/DC converter can be expressed as (2) where $L = L_{arm1}+L_{arm2}+L_t+L_p, R = R_{arm1}+R_{arm2}+R_t+R_p$.

$$v_{abc1} - v_{abc2} = L\frac{i_{abc}}{dt} + Ri_{abc} \quad (2)$$

Apply the DQ transform to (2), the model of converter in DQ frame can be expressed as (3), where $\omega = d\theta/dt$ represents the frequency of the three-phase current i_{abc} and other symbols are defined as (4).

$$\boldsymbol{V_1} - \boldsymbol{V_2} = L\frac{d}{dt}\boldsymbol{I} + \boldsymbol{Z_n}\boldsymbol{I} \quad (3)$$

$$\begin{cases} \boldsymbol{V_1} = \begin{bmatrix} v_{d1} \\ v_{q1} \end{bmatrix}, \boldsymbol{V_2} = \begin{bmatrix} v_{d2} \\ v_{q2} \end{bmatrix} \\ \boldsymbol{I} = \begin{bmatrix} i_d \\ i_q \end{bmatrix}, \boldsymbol{Z_n} = \begin{bmatrix} R & \omega L \\ -\omega L & R \end{bmatrix} \end{cases} \quad (4)$$

It can be seen from the dynamic model of the isolated DC/DC converter that the current flowing through the inductor is driven by the voltage difference of the two MMC converters. Therefore, the concept of common- and difference-mode voltage is introduced here to simplify the model and make it more convenient to design the current and power controllers.

$$\begin{cases} \boldsymbol{V_c} = \frac{1}{2}(\boldsymbol{V_1}+\boldsymbol{V_2}) = [v_{cd}, v_{cq}]^T \\ \boldsymbol{V_d} = \frac{1}{2}(\boldsymbol{V_1}-\boldsymbol{V_2}) = [v_{dd}, v_{dq}]^T \end{cases}$$

By using the definition of common-mode voltage $\boldsymbol{V_c}$ and the difference-mode voltage $\boldsymbol{V_d}$, the dynamic model of the DC/DC converter (3) can be re-written as (5). It can be seen from the dynamic model that, the current of inductor can only be affected by the difference-mode voltage of the converter. Therefore, the current control can be implemented by adjusting the difference-mode voltage $\boldsymbol{V_c}$ of the DC/DC converter, and it can be carried on by a current control loop.

$$2\boldsymbol{V_d} = L\frac{d}{dt}\boldsymbol{I} + \boldsymbol{Z_n}\boldsymbol{I} \quad (5)$$

C. Power Model

According to the instantaneous power theory [11], the instantaneous active- and reactive-power can be expressed as (6).

$$\begin{cases} P = \frac{3}{2}(v_d i_d + v_q i_q) \\ Q = \frac{3}{2}(-v_d i_q + v_q i_d) \end{cases} \quad (6)$$

Because the d-axis of DQ frame is aligned with the current vector, the i_q always equals to 0, therefore, the power from MMC-I to the transformer P_1 and the power from transformer to MMC-II P_2 can be expressed as (7).

$$\begin{cases} P_1 = \frac{3}{2}v_{d1}i_d, P_2 = \frac{3}{2}v_{d2}i_d \\ Q_1 = \frac{3}{2}v_{q1}i_d, Q_2 = \frac{3}{2}v_{q2}i_d \end{cases} \quad (7)$$

If the common-mode voltage $\boldsymbol{V_c}$ is considered with the power model (7), it can be seen that the transmission power of the DC/DC converter can be re-written with the common-mode voltage as (8). Therefore, the transmission power of DC/DC converter are affected by the common-mode voltage and the current at the same time. Therefore, to control the power flow of DC/DC converter, the common voltage and current should be controlled to a specific values at the same time.

$$\begin{cases} P_1 + P_2 = 3v_{cd}i_d \\ Q_1 + Q_2 = 3v_{cq}i_d \end{cases} \quad (8)$$

III. The proposed control method

The control system of the proposed isolated DC/DC converter is shown in Fig. 4. The control system of DC/DC converter consists of three main control loops, the common-mode voltage control loop, the current control loop, and the DC voltage control loop.

The DC/DC converter is responsible for delivering power from the HVDC side to the load side, therefore, the main control object is to control the power flow of the DC/DC converter. According to the direction of power flow, the power injected to the transformer from MMC-I equals to the power received by MMC-II and the power losses, therefore, the power from MMC-I can be express as (9).

$$P_1 = P_2 + P_{loss} \quad (9)$$

It should be pointed out here, the switching losses in not included in the P_{loss} here because it relates to the switching frequency of MMCs. It cannot be affected by the control system, therefore, in this study the switching losses are ignored. The P_{loss} here contains the power losses of resistance of power switches in MMC, resistance of power inductor, the winding losses of transformer, and other elements e.g. cables. Combine (8) and (9) the received power of MMC-II can be expressed based on the common-mode voltage and the current as (10).

$$P_2 = \frac{3}{2}v_{cd}i_d - \frac{1}{2}P_{loss} \quad (10)$$

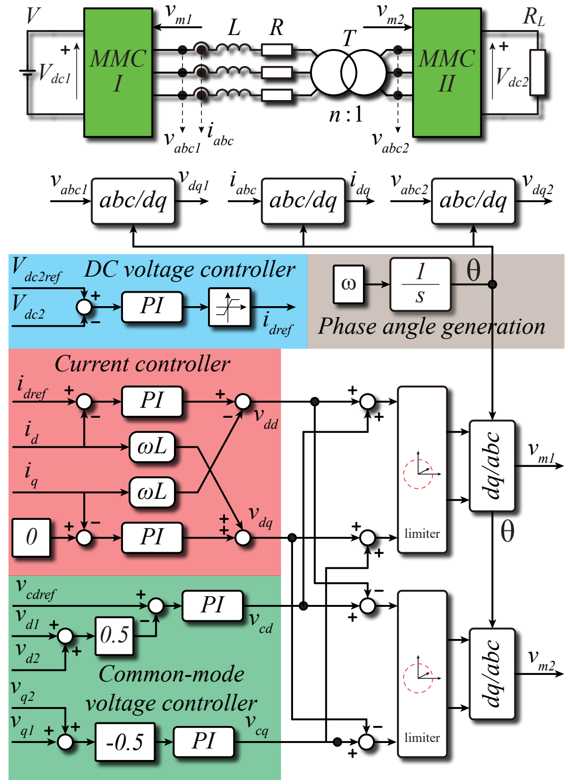

Fig. 4. Control system of the isolated DC/DC converter

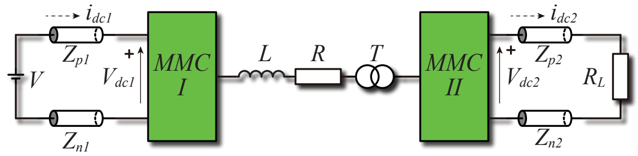

Fig. 5. The test system established in PSCAD for case studies

According to the expression of P_2, the received power by MMC-II can be controlled by adjusting the i_d and v_{cd}. Obviously, the power losses P_{loss} is only affected by the current because of $P_{loss} = Ri_d^2$. Therefore, to reduce the power losses for a specific power delivery P_2, it is better to make the common-mode voltage v_{cd} a constant and as large as possible value so that a smaller i_d can be achieved. However, the common-mode voltage is also limited by the rate voltage of transformers so that it is better to make the common-mode voltage to 1 pu. Consequently, a common-mode voltage control loop is introduced to the control system to obtain a constant common-mode voltage of the DC/DC converter, as shown in Fig. 4.

With a constant common-mode voltage, the received power by MMC-II can be controlled by adjusting the i_d. According to the current model of DC/DC converter (5), the decoupled current controller [12] as shown in Fig. 4 is introduced into the current control loop of the isolated DC/DC converter.

Because the MMC-II is connected to the local island power system, it should provide a constant DC voltage for the local DC/AC converter. By using the current control loop, the power received by MMC-II can be controlled directly. If the power received by MMC-II is larger than the output power, the submodule capacitor in MMC is charging that results in DC voltage increasing of MMC-II. Otherwise, the DC voltage of MMC-II decreases. Therefore, the DC voltage can be controlled by adjusting the power flow from MMC-I to MMC-II. Based on the above analysis, a DC voltage control loop, as shown in Fig. 4 is introduced to the control system to adjust the power received by MMC-II. The DC voltage control loop takes the measured DC output voltage of MMC-II as a feedback signal, and a PI controller is used here to generate the reference value of i_d, based on which the DC voltage control loop can control the power delivery.

IV. Case Studies

To verify the performance of the proposed isolated DC/DC converter for HVDC tapping, a test system shown in Fig. 5 with the proposed control system shown in Fig. 4 is established in PSCAD. The DC/DC converter connected to the main HVDC link represented by an ideal voltage source V through transmission cables labeled as Z_{p1}, Z_{n1}, where the p and n means the positive pole and the negative pole. Moreover, the output of DC/DC converter is connected to a fixed load through transmission lines represented by Z_{p2} and Z_{n2}. The parameters used for the simulation are listed in Table. I.

The simulation results of the DC/DC converter working under steady-state are shown in Fig. 6. The DC voltage from HVDC link is 525 kV, the DC voltage of the low voltage side is 50 kV, and the rate power is 25 MW. To minimize the AC current for reducing the power losses, the common-mode voltage is set to 1 pu. It can be seen from the sub-figure (g) and (h) that the common-mode voltage is controlled to the given reference value, and the difference-mode voltage is established by the current control loop to obtain a 1 pu current flowing through the inductor, as shown in the sub-figure (f). Sub-figure (d) and (e) gives the DQ components of AC voltage generated by MMC-I and MMC-II. It can be seen that the active-power component V_d (blue line) is 1 pu in steady state so that the maximum power delivery can be achieved.

To verify the dynamic response of the DC/DC converter, two kinds of dynamic response are simulated in these case studies. The first dynamic event is a step of voltage reference and the second dynamic event is a load step to present the dynamic performance of the DC/DC converter. For the first dynamic event, a step from 0.9 pu to 1 pu happens at 1 s, and for the second dynamic event, a load step from 0.5 pu to 1 pu occurs at 1.4 s by changing the resistance of R_L. The related results are shown in Fig. 7.

The sub-figure (i) shows simulation results of DC voltage on the low-voltage side, in which the red line is the reference, and the blue line is the output voltage. Before 1s, the output voltage is 0.9 pu and converter works under a normal condition. At 1s, with the reference steps from 0.9 to 1 pu, the DC/DC converter begins to adjust the DC voltage to the reference

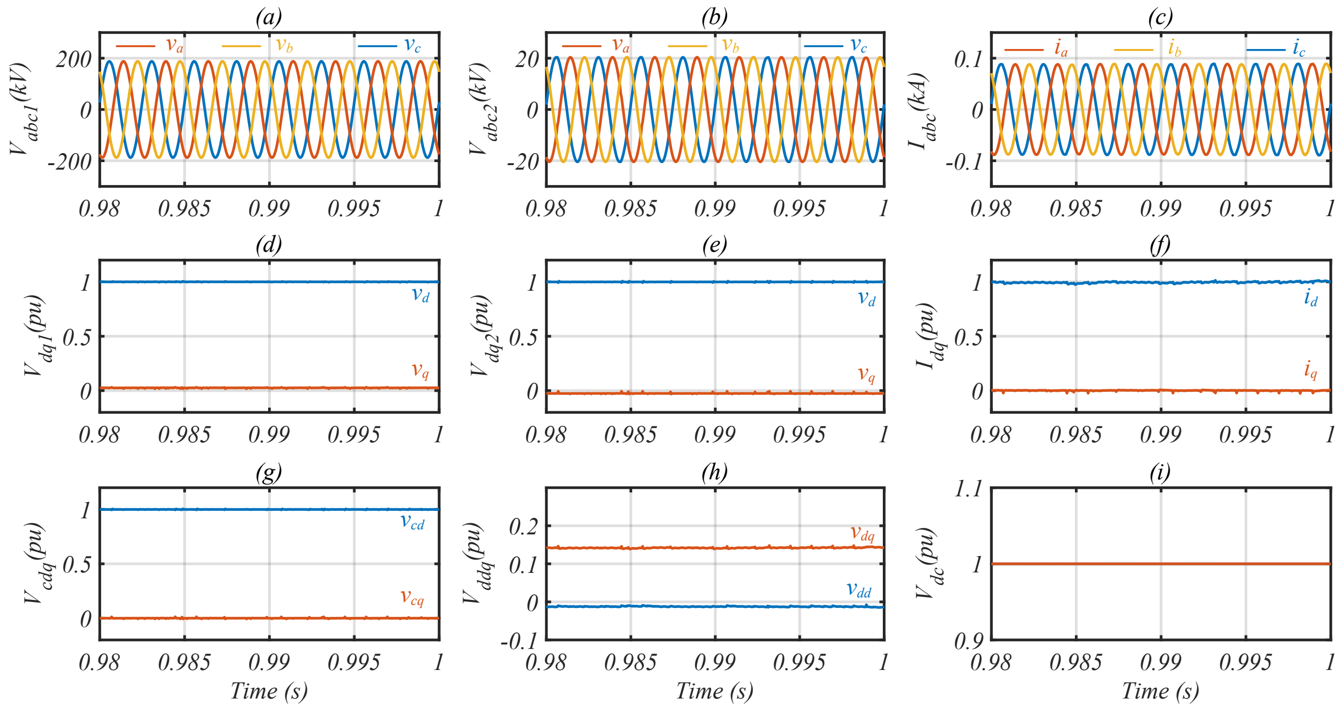

Fig. 6. Simulation results of steady-state conditions. (a) Three-phase voltage of MMC-I AC terminal; (b) Three-phase voltage of MMC-II AC terminal; (c) Three-phase current of inductor L; (d) DQ components of MMC-I AC voltage; (e) DQ components of MMC-II AC voltage; (f) DQ components of AC currents; (g) DQ components of the common-mode voltage; (h) DQ components of the difference-mode voltage; (i) The output DC voltage (V_{dc2}).

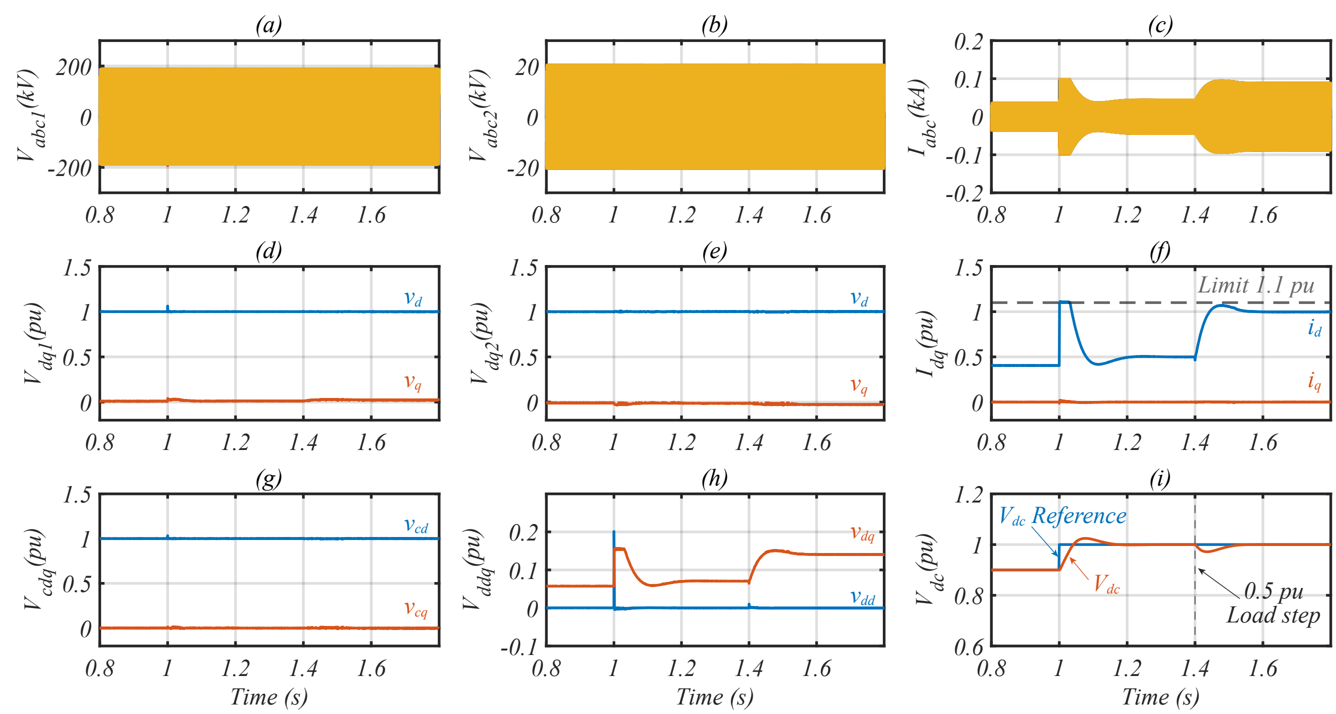

Fig. 7. Simulation results of dynamic response. (a) Three-phase voltage of MMC-I AC terminal; (b) Three-phase voltage of MMC-II AC terminal; (c) Three-phase current of inductor L; (d) DQ components of MMC-I AC voltage; (e) DQ components of MMC-II AC voltage; (f) DQ components of AC currents; (g) DQ components of the common-mode voltage; (h) DQ components of the difference-mode voltage; (i) The output DC voltage (V_{dc2}).

TABLE I
PARAMETERS OF THE TEST SYSTEM FOR SIMULATION

Items		Value
Rate Power S_{base}		25 MW
AC frequency ω		800 π rad/s
Power inductor inductance L		1.5 mH
Power inductor resistance R		10 $m\Omega$
Leakage inductance of transformer X_t		0.05 pu
Winding losses of transformer R_t		0.01 pu
Items	MMC-I value	MMC-II value
Number of SMs per-arm	200	50
DC voltage	525 kV	50 kV
AC voltage	230 kV	25 kV
SM capacitance	4.7 mF	2.2 mF
Arm Inductance	29 mH	1.5 mH
Arm Resistance	20 $m\Omega$	5 $m\Omega$

value and the dynamic response ends after approximately 0.2 s. The sub-figure (f) shows the AC current during the response. At 1 s, because of the reference step, the MMC-II needs more energy to charge capacitors in sub-models, therefore, the AC current increases to deliver more power to the low-voltage side. However, because the power switches in MMC cannot handle the overcurrent, a current limiter is applied to the current control loop, and the current limit is set to 1.1 pu as shown in the sub-figure (f). Thus, when the current increases to the limit, and it keeps unchanged until the output voltage is higher than the reference. It can be seen from the sub-figure (i) and (f), when the output voltage v_{dc} is larger than its reference values, the current decreases quickly from the limit value to the steady-state value. Before 1.2 s, the dynamic response of the current ends and the current reaches to its steady-state value, but at this time the v_{dc} is a little larger than the reference. In reality the current drops to a little less than the steady-state value during transient phase. At the time 1.4 s, a load step is applied to the system by changing the load resistance to half. After the load step, the output power changes to 1 pu suddenly but the received power of MMC-II keeps the value before the load step. At this time, the capacitors in MMC-II release the stored energy to compensate the power unbalance. Therefore, the output voltage reduces after the load step. The output error is detected by the closed-loop power controller and then the power controller adjusts the current reference to deliver more power to the MMC-II to support the voltage. Thus, the current in the sub-figure (f) begins to increase at 1.4 s. The adjusting time of the power controller is approximate 100 ms, which is represented by the current shown in sub-figure (f). It can be seen that after approximate 100 ms, the current reaches its steady-state value 1 pu. It has to be pointed out here that in the second dynamic event, there does not have overshot in the voltage response. This is because the current does not reach its limit value, and the voltage controller is tuned to a typical first-order system.

V. CONCLUSION

HVDC tapping technology maybe a convenient solution for archipelago power systems to provide stable and high-quality electric power for power systems of small islands. To meet requirements of HVDC tapping technology, this paper proposes a potential MMC-based isolated DC/DC converter for the HVDC tapping. This paper first studied the mathematical model of the MMC-based isolated DC/DC converter by using the concept of common-mode and difference-mode voltages. It shows that the mathematical model of the isolated DC/DC converter can be simplified for the control system design by introducing the common- and difference-mode voltage. Based on the developed model, a control system of the DC/DC converter, including the decoupled current controller and the voltage/power controller is proposed. The simulation results indicates that the proposed method is satisfactory for output voltage steps and load steps and the dynamic response is fast. By using the common-mode and difference-mode voltage, the control system is more flexible to gain a better performance. With the proposed control system, the converter has acceptable steady-state and dynamic performance which is verified by the simulation in PSCAD. However, the proposed method can be further improved by 1) considering the power balance between two MMCs; 2) optimizing the parameters of the controller; and 3) considering the fault ride through control strategy, which are focused of our further research.

REFERENCES

[1] Ministry of Energy and Mineral Resources, “Indonesia Grid Code 2022 (Permen ESDM No.20 2020),” 2020. [Online]. Available: https://jdih.esdm.go.id/storage/document/PM%20ESDM%20No%2020%20Tahun%202020.pdf.

[2] Institute for Essential Services Reform, “Indonesia Energy Transition Outlook 2021,” 2021.

[3] R. Irnawan and F. M. F. da Silva, “The HVDC Green Handbook,” Aalborg, 2022.

[4] T. K. Vrana et al., “The CIGRE B4 DC grid test system”, pp. 10-19, Oct. 2013.

[5] D. Jovcic and H. Zhang, “Dual Channel Control With DC Fault Ride Through for MMC-Based, Isolated DC/DC Converter,” IEEE Trans. Power Delivery, vol. 32, no. 3, pp. 1574-1582, June 2017, DOI: 10.1109/TPWRD.2017.2675909.

[6] S. Kenzelmann, A. Rufer, D. Dujic, F. Canales and Y. R. Novaes, ”Isolated DC/DC structure based on modular multilevel converter”, IEEE Trans. Power Electron., vol. 30, no. 1, pp. 89-98, Jan. 2015.

[7] A. Garcia-Bediaga, I. Villar, A. Rujas, I. Etxeberria-Otadui, A. and Rufer, “Analytical models of multiphase isolated medium-frequency dc-dc converters”, IEEE Trans. Power Electron., vol. 32, no. 4, pp. 2508-2520, Apr. 2017.

[8] B. Zhao, Q. Song, J. Li, Y. Wang and W. Liu, “High-Frequency-Link modulation methodology of DC-DC transformer based on modular multilevel converter for HVDC application: Comprehensive analysis and experimental verification”, IEEE Trans. Power Electron., vol. 32, no. 5, pp. 3413-3424, May 2017.

[9] T. Luth, M. M. C. Merlin, T. C. Green, F. Hassan and C. D. Barker, “High-frequency operation of a DC/AC/DC system for HVDC applications”, IEEE Trans. Power Electron., vol. 29, no. 8, pp. 4107-15, Aug. 2014.

[10] A. Jamshidifar, M. Hajian, D. Jovcic and Y. Audachya, “High power MMC VSC optimal design for DC/DC converter applications”, IET Power Electron., vol. 9, no. 2, pp. 247-255, Feb. 2016.

[11] T. Furuhashi, S. Okuma, and Y. Uchikawa, “A study on the theory of instantaneous reactive power,” IEEE Trans. Ind. Electron., vol. 37, no. 1, pp. 86-90, Feb. 1990.

[12] Q. Zhang, D. Liu, Z. Liu and Z. Chen, ”Fault modeling and analysis of grid-connected inverters with decoupled sequence control”, IEEE Trans. Ind. Electron., Jun. 2021.